Pedagogical Lectures on MBL

John Z. Imbrie

University of Virginia

ICTS Bengaluru
January, 2024

The Plan

Lecture 1: *Analytical tools for a proof of Anderson localization*
Lie-Schwinger rotations provide a graphical framework for stepwise diagonalization of the Hamiltonian. Nonperturbative regions are controlled probabilistically with moment estimates and the Markov inequality.

Lecture 2: *Existence of an MBL phase*
I will describe competing effects on the density of nonperturbative regions. In the RG, isolated nonperturbative regions can be eliminated, while nearby ones have to be merged. Percolation estimates ensure that these regions are compact and rare, maintaining a minimum exponential decay rate and forestalling the avalanche mechanism.

Lecture 3: *The MBL transition*
In order to understand the nature of the transition between the MBL and ETH phases, I will use a series of approximations to develop RG flow equations based on elimination and merging of nonperturbative regions. These equations resemble the Kosterlitz-Thouless (KT) flow equations, but there are important differences that place the MBL transition in a new universality class.

Outline of Lecture 1[1]

1. The Anderson model
2. Resonant set
3. Schrieffer-Wolff rotations
4. Graphical analysis
5. Block rotations and buffer zones
6. Graphical analysis in the k^{th} step
7. Fractional moment bounds and Markov inequality
8. Long graphs and the forward aproximation
9. Conclusions

[1] Based on my paper "Multi-scale Jacobi method for Anderson localization", CMP2016

The Anderson Model

On a rectangle $\Lambda \subset \mathbb{Z}^d$ we define

$$H = H_0 + J$$

$$H_{0,xy} = v_x \delta_{xy} \equiv E_x \delta_{xy}$$

where v_x is a random potential $\equiv$ "unperturbed energies" on the lattice, iid, with smooth distribution.

$$J_{xy} = \begin{cases} -J_0, & |x - y| = 1; \\ 0, & \text{otherwise.} \end{cases}$$

We take $J_0 \ll 1$.

Resonant Set

In the first step we put

$$S_1 = \{x \in \Lambda : x \text{ is in a resonant pair, } \textit{i.e. } |v_x - v_y| < \varepsilon\},$$

where

$$\varepsilon = J_0^{1/20}.$$

We can see that S_1 is a dilute subset of Λ. We don't do Schrieffer-Wolff rotations in S_1, at least initially.

Schrieffer-Wolff rotation

We put

$$\Omega = \exp(-A)$$

where

$$A_{xy} = \frac{J^{\mathrm{per}}_{xy}}{E_x - E_y},$$

where J^{per}_{xy} is J_{xy} if both x and y are outside S_1, and 0 otherwise. It represents the "perturbative" hopping terms that move between nonresonant sites.

Note that $|A_{xy}| \leq J_0^{19/20}$

We may put $J = J^{\mathrm{res}} + J^{\mathrm{per}}$, the sum of resonant and perturbative pieces.

Schrieffer-Wolff rotation, cont.

Then, using $H = H_0 + J$, we have $[A, H] = -J^{\mathrm{per}} + [A, J]$, and so

$$
\begin{aligned}
H^{(1)} &= e^{A} H e^{-A} = H + [A, H] + \frac{[A, [A, H]]}{2!} + \dots \\
&= H_0 + J^{\mathrm{res}} + J^{\mathrm{per}} - J^{\mathrm{per}} + [A, J] + \frac{[A, -J^{\mathrm{per}} + [A, J]]}{2!} + \dots \\
&= H_0 + J^{\mathrm{res}} + \sum_{n=1}^{\infty} \frac{(\mathrm{ad}A)^n}{n!} J - \sum_{n=1}^{\infty} \frac{(\mathrm{ad}A)^n}{(n+1)!} J^{\mathrm{per}} \\
&= H_0 + J^{\mathrm{res}} + \sum_{n=1}^{\infty} \frac{n}{(n+1)!} (\mathrm{ad}A)^n J^{\mathrm{per}} + \sum_{n=1}^{\infty} \frac{(\mathrm{ad}A)^n}{n!} J^{\mathrm{res}} \\
&= H_0 + J^{\mathrm{res}} + J^{(1)}. \qquad (1)
\end{aligned}
$$

Here $\mathrm{ad}A = [A, \cdot]$.

Graphical analysis

Graphically, we obtain a walk g in $\mathbb{Z}^d$ along with energy denominators $1/(v_x - v_y)$, here drawn as arches (in the first step only nearest-neighbor denominators appear):

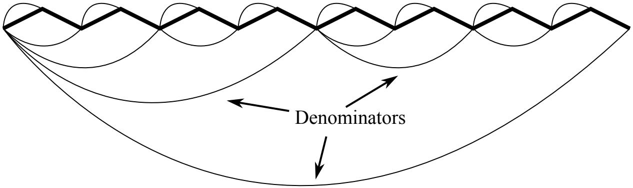

We obtain that

$$|J_{xy}^{(1)}(g_1)| \le J_0 (J_0/\varepsilon)^{|g_1|-1}$$

"Renormalized" interactions are no longer nearest-neighbor, but they decay exponentially.

Block Rotations

Let $\bar{S}_1$ be S_1 plus its first neighbors in the lattice.
Divide its components into small (volume $\leq \exp(M2^{2/3})$) and large ($\geq \exp(M2^{2/3})$).

As in quasidegenerate perturbation theory, we apply rotations in small blocks to diagonalize the Hamiltonian there.

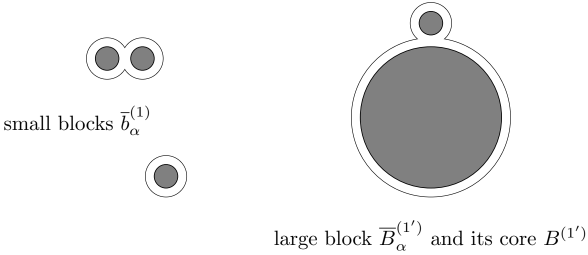

The shaded region is S_1, the resonant set. $\overline{S}_1$ includes the collar regions.

Blocks in later steps; buffer zones

In subsequent steps, small blocks will have volume $\leq \exp(ML_k^{2/3})$ with $L_k = (15/8)^k$.

This will ensure that the exponential decay $(J_0/\varepsilon)^{L_k}$ will keep the sum over states in the block under control.

Residual interactions between a block and its collar are not under perturbative control (this is the reason for the collar). In the many-body context, it is connected to the thermalization of collar neighborhoods of resonant regions.

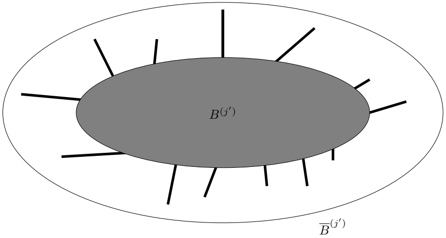

Leftover interaction terms couple the core $B^{(j')}$ to its collar.

Graphical analysis in the k^{th} step.

We use a sequence of length scales $L_k = (15/8)^k$, and in each step we rotate away interactions of lower order than $J_0^{L_k}$.

This is Newton's method in action; if a term of order L_k is rotated away, it creates new terms of order $2L_k$ or more.

Graphical analysis in the k^{th} step., cont.

In each step $J^{(k)\text{per}}$ is a sum of connected graphs $J^{(k)}_{xy}(g)$; with exponential decay.

Each graph g is a walk in $\mathbb{Z}^d$ with associated energy denominators.

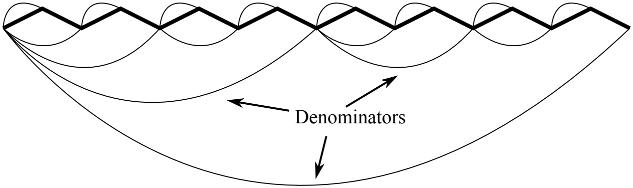

A graph of order L_k is said to be resonant if two conditions hold:

1. $A^{(k)}_{xy}(g) \equiv \frac{J^{(k)}_{xy}(g)}{E^{(k)}_x - E^{(k)}_y}$ is larger in magnitude than $(J_9/\varepsilon)^{|g|}$.
2. $|x-y|^{(j)} \geq \frac{7}{8}|g|$, where $|\cdot|^{(j)}$ is the metric where blocks on scales up through j are contracted to points.

It is important to maintain comparability of this metric with the usual one throughout the procedure.

Fractional moment bounds and Markov inequality

Use fractional moment bounds to control the probability of a resonant graph, i.e.

$$\mathbb{E}\left|A_{xy}^{(k)}(g)\right|^s \leq J_0^{|g|} \prod_I \int \frac{dv_i}{|v_i - v_j|^s} \leq |CJ_0|^{|g|}.$$

Here s is the fractional moment, it must be less than 1 for finiteness of the integral.

Then the Markov inequality implies that

$$\left|A_{xy}^{(k)}(g)\right|^s \leq |CJ_0/\varepsilon|^{|g|} \text{ with probability } 1 - \varepsilon^{|g|}$$

However, this assumes each site is different (forward approximation).

Long graphs and the forward approximation

If there is significant backtracking, we don't use Markov inequality; instead we get extra decay compared with $|x - y|$ (a walk with repeated sites can't travel as far – see next slide).

With this bound on the probability of a resonant graph, it is OK to sum over $\exp(O(L_k))$ graphs in the associated percolation problem with $L_{k-1} < |g| \leq L_k$.

Percolation clusters = new resonant blocks:
They are the connected components of the set of resonant graphs in space

Backtracking graphs

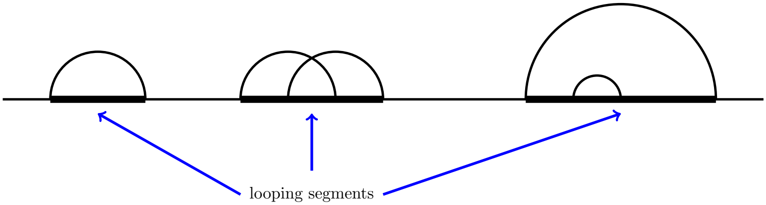

Timeline of the walk. Arches connect pairs of times where the walk is at the same site/block.

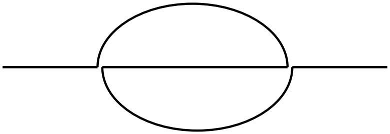

A walk executing loops exhibits triple connectivity.

Result on exponential localization

We prove exponential decay of the eigenfunction correlator for small J_0.

Theorem

The eigenvalues of $H^{(\Lambda)}$ *are nondegenerate, with probability 1. Let* $\{\psi_\alpha(x)\}_{\alpha=1,\dots,|\Lambda|}$ *denote the associated eigenvectors. There is a* $\kappa > 0$ *such that if* J_0 *is sufficiently small, the following bounds hold for any rectangle* Λ*. The eigenfunction correlator satisfies*

$$\mathbb{E} \sum_\alpha \left|\psi_\alpha(x)\psi_\alpha(y)\right| \leq J_0^{\kappa|x-y|}, \text{ and consequently}$$

$$\sum_\alpha \left|\psi_\alpha(x)\psi_\alpha(y)\right| \leq J_0^{\kappa|x-y|/2} \text{ with probability } 1 - J_0^{\kappa|x-y|/2}.$$

Proof: Concatenate the rotation matrices produced in the course of the analysis. We know the graphs exhibit exponential bounds outside the resonant regions. The resonant regions are based on graphs that don't obey exponential bounds, but we obtain exponential decay under the expectation, as their probabilities decay exponentially. The result follows by combining the "probability graphs" with the rotation graphs.

Conclusion

This paper was developed as a warm-up exercise for the MBL problem. We will see in my next lecture how the ideas are adapted for the MBL proof.

The key issue that I needed to address was the lack of exponential bounds on probabilities in multi-scale analysis (MSA) proofs of localization. The best MSA bounds prior to this work gave at best stretched exponential, which clearly would never be sufficient to control exponential state sums in the MBL problem.

Note: exponential bounds such as the above theorem were previously proven using the fractional moment method of Aizenman-Molchanov. However, that method did not appear flexible enough to use in the MBL problem.